投稿論文(英文)
PAPERS

Proc. of JSCE No. 451/V-17, pp. 245~253, August 1992

EFFECT OF STATE OF STRESS AT THE GRIPS AND MATRIX PROPERTIES ON TENSILE STRENGTH OF CFRP RODS

Hosam HODHOD* and Taketo UOMOTO**

The problem of double peak tensile strength distribution for CFRP rods, 8), is investigated. First, single carbon fibers were tested in tension and the strength distribution was obtained. Consequently, a model for tensile failure of CFRP rods was proposed, assuming ideal matrix properties. The actual behaviour of the rods was compared with the ideal one in order to determine the deviation in behaviour. The reliability of the measured strains was ensured through two types of experiments, that led, also, to characterisation of the loading system. The picture was completed by testing the binding matrix together with two other matrices for comparison and the results of all the previous experiments were analysed. The analysis assures the importance of the large matrix strain capacity for maintaining rods high strength.

Keywords : *FRP, tensile failure, statistical distributions, fiber testing, prestressing tendons*

1. INTRODUCTION

Statistical characterisation of engineering materials is very important for providing useful and necessary information about them. The common use of distribution curves is for extracting appropriate safety factors for specific material and specific application. In case of new materials, *e.g.* FRP, material behaviour is investigated through this statistical analysis. The distribution gives mean value, scattering of the strength and, in addition, might indicate more than one dominant failure behaviours. In the latter case, investigation of the material constituents, if more than one exist, becomes the key approach to the clarification of such phenomenon. Other factors like loading configuration and manufacturing process might have significant effect too.

One of the up-to-date materials is the FRP in forms of rods for prestressing tendons of concrete. Many fiber-matrix combinations are used for these rods. This research considers the behaviour of carbon FRP rods under static tensile loading ; which is the fundamental case of loading encountered in practice. However, the argument given herein is also applicable, conceptually, to other kinds of FRP rods and related work, performed by the authors, will be mentioned in time.

2. CFRP RODS TENSILE TESTING FOR STRENGTH CHARACTERISATION (PROBLEM EVOLUTION)

* Doctoral Student, Institute of Industrial Science, University of Tokyo (MINATO-KU, TOKYO 106, JAPAN)
** Professor Institute of Industrial Science, University of Tokyo

As explained in reference 8), one hundred CFRP rods, each of total length 40 cm and diameter 6 mm, were tested in static tension. The testing was of the hard system (displacement control) with cross-head speed 2 mm/min. The testing machine was Autograph with capacity of 10 tons. The rods had fiber volume fraction (V_f) of 0.66 and epoxy acrylate resin matrix (*Ripoxy H-600*). Rods surfaces were smooth and, in order to grip them, rods ends were coated using an adhesive and iron powder. This coating was let cured for at least one day before testing. The grips were those introduced by Kobayashi[5], and composed of two inner conical wedges holding the rod, and guided by outer sleeve of cylindrical outer surface and conical inner surface. The grips are shown in **Fig.6** (b).

The nominal strength of the rods was calculated through dividing failure load by the total cross sectional area. The strength cumulative probability is plotted in **Fig.1** (a) where two regions can be seen evidently. Strength data was divided into two categories, strengths less than and above 160 kg/mm^2, and the two distributions are shown in **Fig.1** (b). The corresponding Gaussian density functions were combined into the two-peak density function shown in **Fig.1** (c). The two peaks indicate two different failure mechanisms and for clarification, the following experimental work was performed. It should be mentioned that all the rods were taken from the same batch, and there was no correlation between tensile strength and curing period for end coating.

3. EXPERIMENTAL WORK AND RESULTS

(1) Tensile Tests for Carbon Fibers

Fibers used for rods reinforcement were tested in

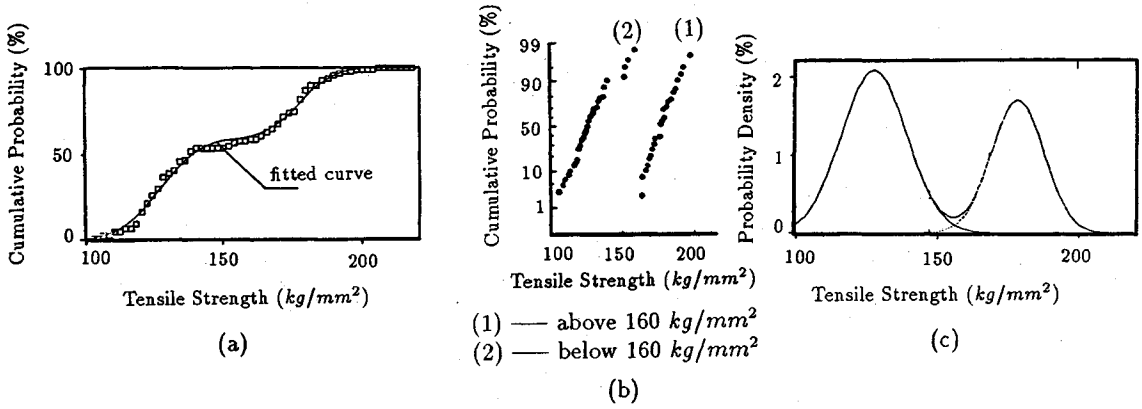

Fig.1 Tensile Strength Distributions for CFRP Rods[8]

static tension. Single fibers were separated from different locations along fibers spool, and each fiber was attached individually to a standard piece, (JIS R-7601/1986), of section paper as shown in **Fig.2**. The test was of the hard system and three rates of loading were used (corresponding to cross-head speeds of .4, 1.0 and 3.3 mm/min.). Fifty specimens were tested at each loading rate, and load-displacement curves for all specimens were linear.

In order to calculate the stress accurately, fibers diameters were measured using the scanning electron microscope (SEM). One hundred pieces of data were collected from different sections along different fibers. The cumulative distribution of the diameters and its statistical parameters are given in **Fgi.3**. The low scattering allows the use of mean diameter for statistical evaluation of fibers strength. Fibers uniformity is assured through scanning electron micrographs, as shown in **Fig.4**.

The mean strength for each loading rate was calculated and no significant effect, for loading rate, was detected. Therefore, all the data, regardless of loading rate, was used for strength analysis. Probability density and cumulative probability for experimental data, and the corresponding Weibull functions[9),4)] are given in **Fig.5**. Stress- strain relationships, concluded from load-displacement curves, are essentially linear, and the calculations of maximum strain and Young's modulus are straight forward. Mean values for tensile properties are given in **Table 1**.

Based on the previous results, a model[3)] for CFRP rods behaviour in tension was proposed. The model assumes negligible matrix strength compared with fibers strength, perfect fiber-matrix bond, and rigid-plastic matrix behaviour upon fibers failure. Hence, the ideal stress-strain relationship for the rods is linear up to failure. An

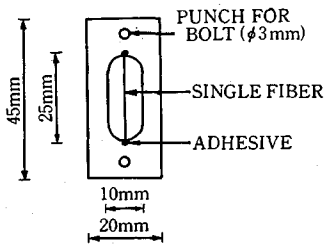

Fig.2 Standard Specimen for Fibers Tests

Table 1 Tensile Properties for Carton Fibers

Tensile Strength (kg/mm²)	max. Strain (%)	Young's Modulus (kg/mm²)
335	1.380	22700

estimation for mean rods strength was given as that corresponds to fibers stresses equal to the mean strength of fibers.

(2) Strain Gages Reliability Tests

In order to compare actual behaviour of the rods and the ideal one[3)], representative stress-strain curves for the rods should be obtained. Strain gages are usually attached to the rods at the center. However, due to the small gage length, the strain at the center might be significantly different from that elsewhere. In order to investigate the reliability of strain gages measurements, two types of experiments were performed. In the first one, the strain gages were attached to five different locations along the rods : at the center (c) and at 7.5 and 20 mm from each chuck (U_1 & U_2 and l_1 & l_2). In the second set of experiments, the different displacements in the loading system were monitored in addition to measuring the strains at the center using resistance strain gages and clip gage. The overall rod response is calculated as the difference between the cross-head displacement and the losses

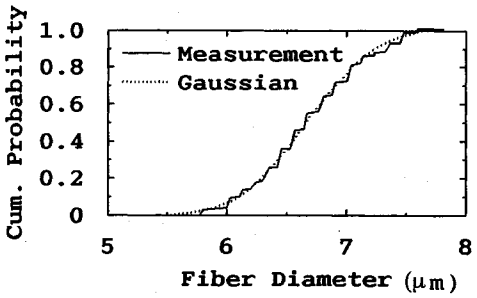

Fig.3 Carbon Fibers Diameters Distribution

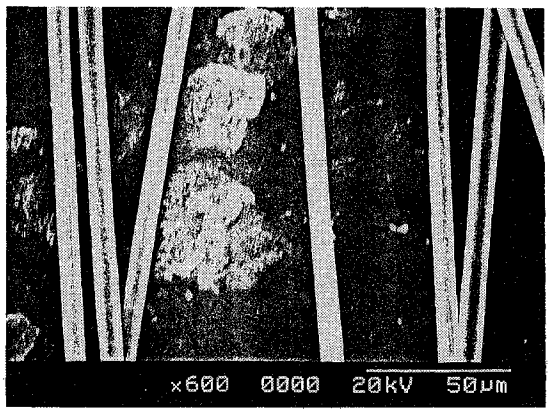

Fig.4 Uniformity of Carbon Fibers (SEM photo ×600)

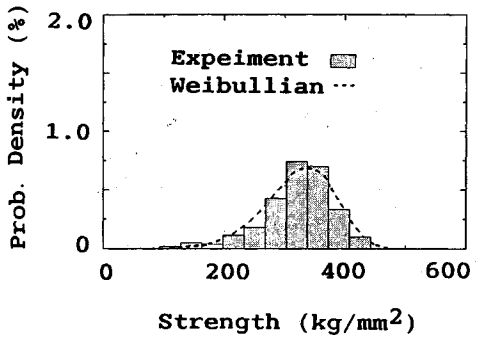

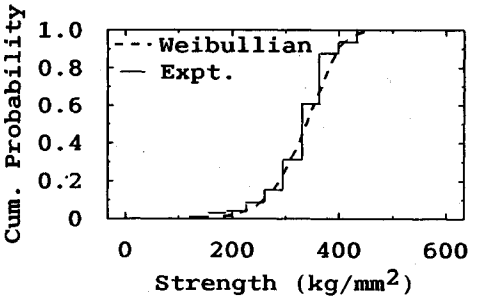

meam=335 kg/mm²
standard deviation=52 kg/mm²
Weibull modulus=7.5

Fig.5 Tensile Strength Distribution for Carbon Fibers

in the loading system. **Fig.6** (a) shows the rods loading configuration and **Fig.6** (b) shows photograph for the gripping chucks and schematic representation for the chuck zone at two successive loading stages.

When the cross-head is lowered, load is applied to the system and as each of the elements has stiffness, they will respond to this acting load and consume part of cross-head displacement. **Fig.6** (c) shows mechanical model for loading system. The connection S_l between the lower chuck and cross-head, and also that, S_u, between the upper chuck and the girder, are stiff springs. The response of S_l, relative displacement, can be measured by connecting transducer between the cross-head and the outmost chuck. The response of S_u can be measured by transducer connected to the upper outmost chuck from any fixed object (*e.g.* machine post).

As regards shuck zone, **Fig.6** (b), the inner block moves during loading from one position A to deeper position B in order to provide the lateral pressure required to grip a rod stretched with load P. There exist two probable slip surfaces : Sr_1 and Sr_2. However, the surface Sr_2 was made more rough through coating with adhesive and iron powder.

Hence, the slip from A to B occurs mainly on the surface Sr_1. The response of chuck zone can be measured using PI-gage connected as shown in **Fig.6** (d). The only left response is, then, that of the rod (i.e. relative displacement between rod ends). All responses in the loading system are, hence, related as follows

$$U_t = U_{su} + U_{sl} + U_{cu} + U_{cl} + \Delta L_r \cdots\cdots (1)$$

where U_t=cross-head displacement
U_{su}=response of the connection S_u
U_{sl}=response of the connection S_l
U_{cu}=total slip at the upper chuck
U_{cl}=total slip at the lower chuck
ΔL_r=total elongation of the rod

and

$$\Delta L_r = \int_l \epsilon dl = \epsilon_c L_r \cdots\cdots (2)$$

(if the central strain ϵ_c is representative to the overall strain)

Sample output for the first experiment is shown in **Fig.7** where all the strains measured, using the strain gages, at different sections agree well. As regards the second experiment, **Fig.8** shows the variation of different responses, and **Fig.9** shows the rod strains measured at the center using strain gage (gage length 2 mm) and clip gage (gage length 50 mm) and the calculated strains from equation

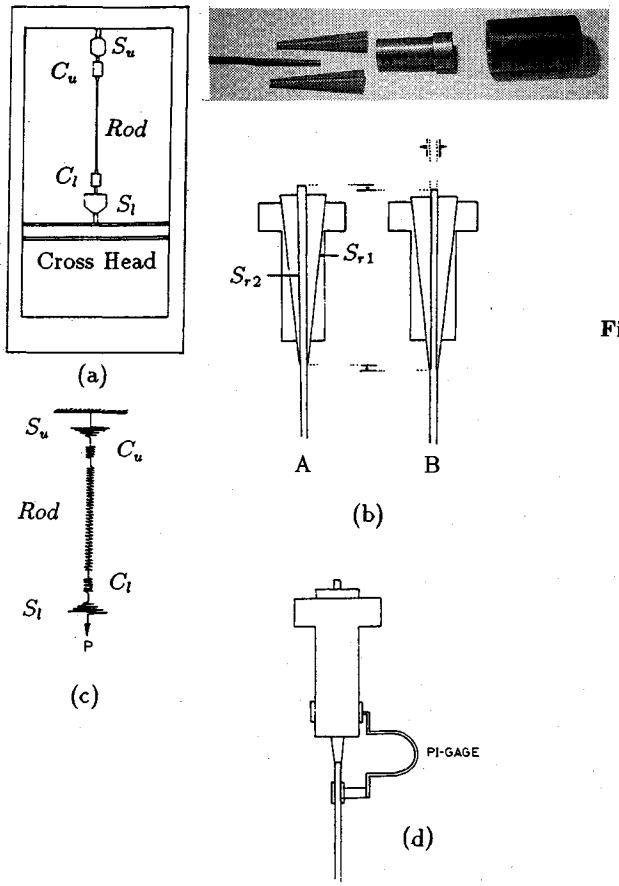

Fig.6 (a) Rod Loading Configuration
(b) Gripping Chucks
(c) Mechanical Model for Loading System
(d) PI-Gage Installation

(1). The good agreement of the measurements and calculations is evident.

(3) Strain Monitored CFRP Rods Tensile Testing

In order to get the actual behaviour of the rods, 20 CFRP rods each of total length 40 cm and diameter 6 mm, were prepared for testing as in reference 8). Two resistance strain gages were attached to opposite sides at the center of each rod. The strain gages and load output terminal, of the testing machine, were connected to a data logger for data recording. The stress-strain relationships for all specimens were obtained and the failed rods were visually inspected for any common feature. Samples of the stress-strain curves are given in **Fig.10** and a photograph for the typical failure is shown in **Fig.11**. The agreement of the actual rod behaviour and the model[3] up to failure start is evident for all specimens. Similar agreement for other FRP rods, namely : glass and aramid FRP rods, was also reported in jontly performed

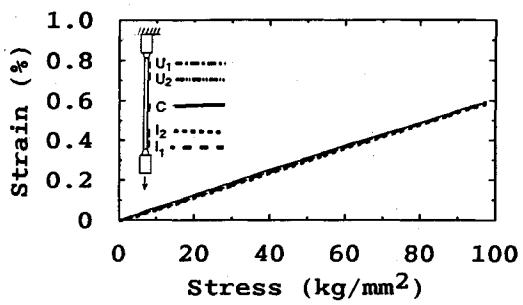

Fig.7 Longitudinal Strains at Different Sections along the Rod

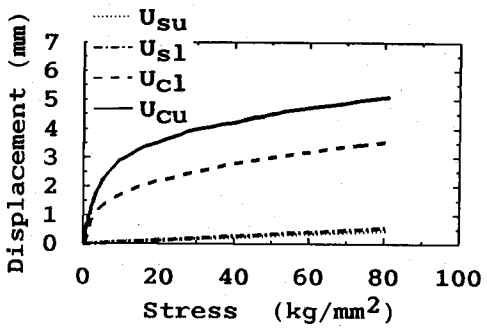

Fig.8 Variation of Different Responses

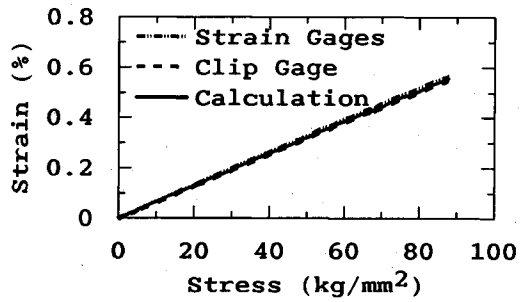

Fig.9 Calculated and measured Strains

experiments.

(4) Tensile Tests for Matrix

In order to complete the data about the behaviour of rods constituents, the matrix was tested in static tension. Other two different matrices used for FRP rods were also tested for comparison. Three specimens of each matrix were prepared according to JIS K-7113/1981 (*type 1*). Resistance strain gages, for axial and transverse strains measurements, were attached to both surfaces of each specimen at the center. For all experiments, the crosshead speed was 2 mm/min. Tensile strength, maximum strain, initial tangent modulus of elasticity and Poisson's ratio are given for all matrices in **Table 2** (average of the three specimens). Typical stress-strain relationships for the

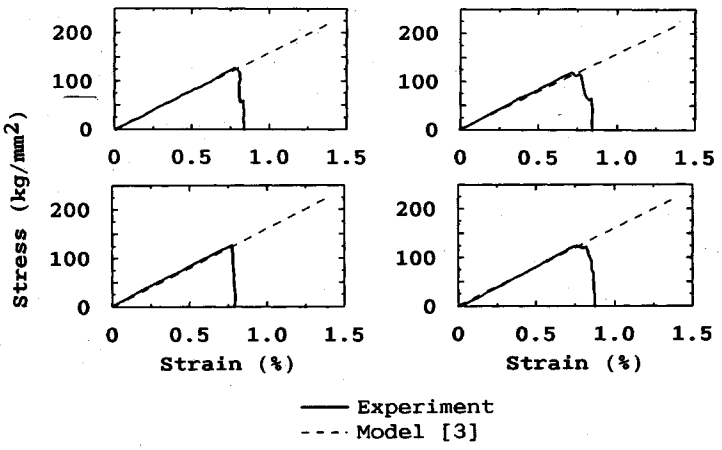

Fig.10 Samples of Stress-Strain Relationships for CFRP Rods

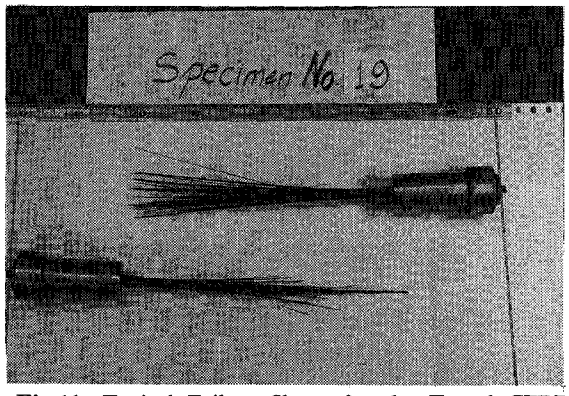

Fig.11 Typical Failure Shape for the Tested CFRP Rods

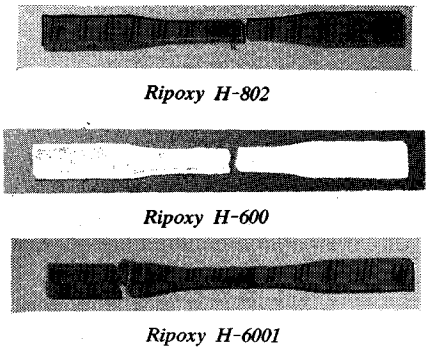

(b)

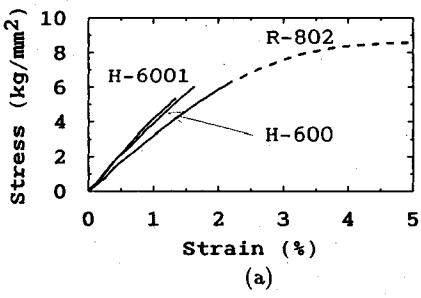

(a)

Fig.12 (a) Stress-Strain Relationships for the Tested Matrices.
(b) Failure Shape for the Tested Matrices.

Table 2 Tensile Properties for different Matrices

Matrix	Tensile Strength (kg/mm²)	max. Strain (%)	Young's Modulus (kg/mm²)	Possion's Ratio
Ripoxy R-802	6.44 (8.60)	2.2 (5.0)	315 (320)	.335
Ripoxy H-600	6.50	1.9	400	.350
Ripoxy H-6001	5.60	1.4	430	.340

Values in parantheses represents the broken curve in Fig. 12

three matrices are shown in **Fig.12** together with photographs for the failed specimens. The broken extension for the stress-strain curve of *Ripoxy R-802* is obtained from the producer because the tested specimens, continuous line, contained initial cracks and did not exhibit the full strain capacity (but still tracing the same curve).

4. DISCUSSION

In the strain gage reliability experiments (first one), the agreement of the measurements at all sections assures the fact that load transfer from the chucks to the rod is completed within chuck length. It also confirms the argument made for the model[3] that the individual fiber failures at different sections does not affect the overall rod response and the severe damage of fibers takes place rarely along the rod, before final rod failure.

In the second experiment, the agreement of the measured and calculated strains indicates that

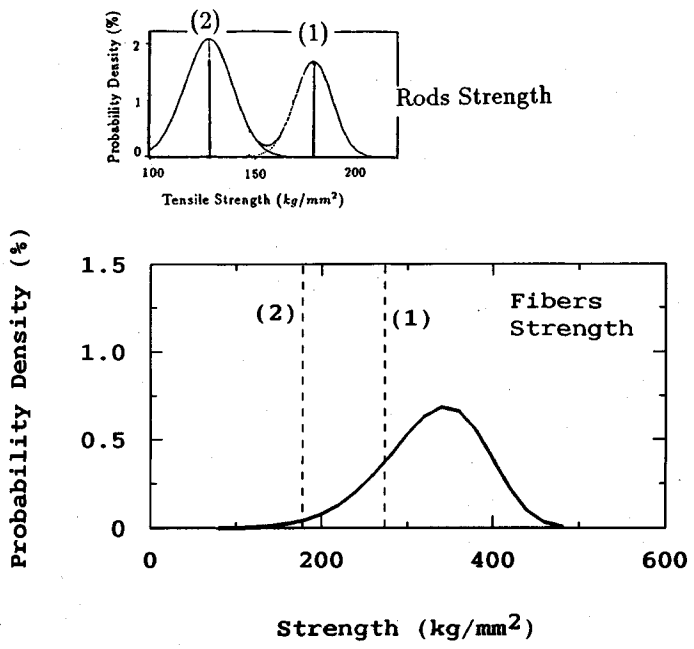

Fig.13 Fibers Stresses at the Two Peaks of Rods Strength Distribution

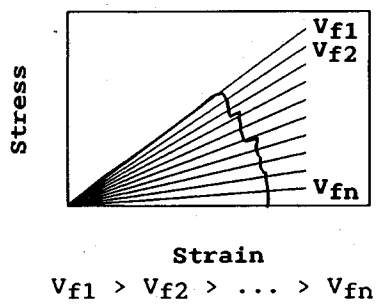

Fig.15 Failure Path on Idealized Curves with Lower Fiber Volume Fractions

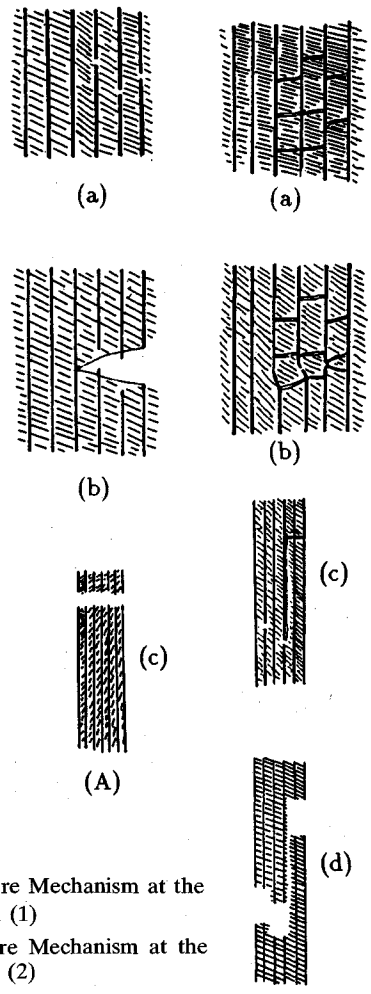

(A) Failure Mechanism at the High Peak (1)
(B) Failure Mechanism at the Low Peak (2)

Fig.14

resistance strain gages, in spite of their short length, represent satisfactorily the overall response of the rods, and hence their use in monitoring the strains of rods is sufficiently reliable for evaluating rods behaviour.

The measurements from PI-gages indicate the lateral pressure, exerted by chucks, on rods ends during loading. This effect, as will be shown later, leads to reduction of rods strength.

In tension experiments on matrices, failure shape, **Fig.12** (b), shows the sensitivity of the brittle matrix (*H-6001*) to the lateral pressure from grips. The similarity between the stress-strain curves of this matrix and (*H-600*) indicates the potential of *H-600* to fail within the grips if additional lateral pressure is exerted.

In order to give interpretation for the two peaks of rods strength distribution, **Fig.1** (c), the stress of the fibers at each peak is calculated. This stress is 1.5 times rods stress ($V_f = .66$). The two stress levels are plotted on fibers strength distribution, as shown in **Fig.13**. The stress at the low peak (2) lies at the left end of the distribution. This indicates that the failure was not initiated by fibers failure, as the typical failure process in fibers composites[2),4)]. On the contrary, the stress at the high peak (1) lies inside the distribution where the failure of reasonable number of fibers is possible and hence the typical failure process is likely to take place. This typical process is illustrated in **Fig.14** (A) ; where some fibers fail first causing the evolution of weak spot inside the material (a). The failure extends to the surrounding matrix resulting in a crack-like defect. The defect propagates to the neighbour fibers (b), due to the high nominal stress level and additional stresses from the defective zone. In (c),

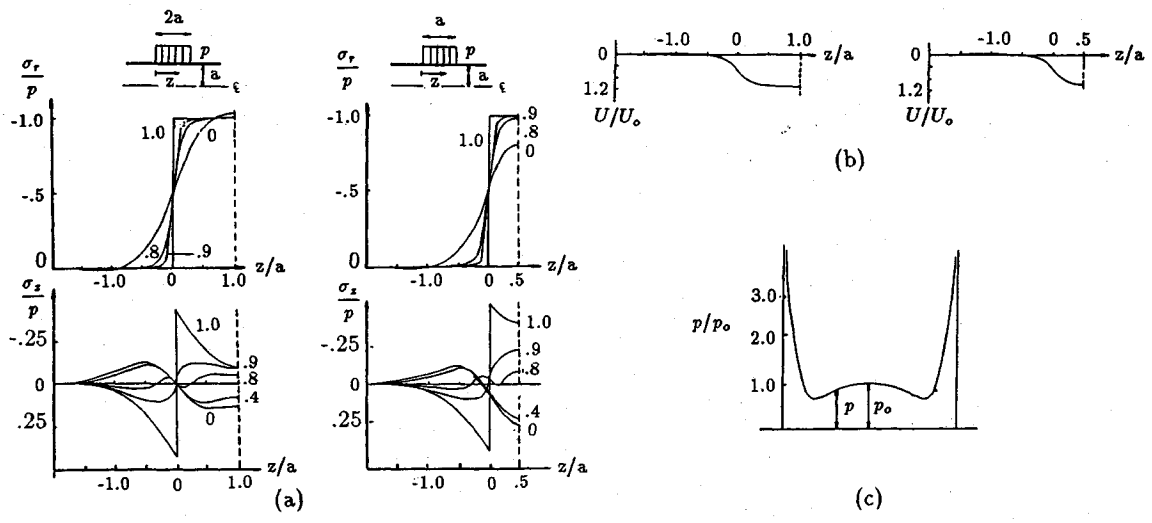

Fig.17 (a) Radial and Axial Stresses Distributions, for Different r/a, in a Cylinder Uniformly Loaded along Lengths a and 2 a of the Surface[1)]
(b) Radial Surface Displacements for the Loadings in (a)[1)]
U_0=Radial Surface Displacement Due to Uniform Pressure along the Whole Surface.
(c) Loading for Uniform Radial Displacements over Length a[1)]

failure is completed, more or less, at the same section by further propagation of the defective zone.

The proposed failure mechanism for the low peak is shown in **Fig.14** (B). In view of matrix properties discussed above, the matrix fails first (a) under the effect of both axial and lateral stresses at the grips. Under the effect of the lateral pressure from the grips, the failed matrix causes the failure of the neighbour fibers in modes like shear and crushing (b). Again, the defective zone evolutes, as in (1), but extends in different direction. Due to the low stress level and the existence of defective matrix, the failure is more likely to propagate in debonding mode along the rod (c). This connects the weak zones at different sections and causes, instantaneously, reduction in the effective volume fraction of the rod, and hence in its response to the applied loading process. In (d), the failure is completed by breakage of the left sound fibers and by pullout mechanism resulting in an irregular shape for the failed rods.

The rods tested in this research showed strengths in the range of the lower peak and their failure shape is irregular as shown in **Fig.11**. Also, their stress-strain curves exhibited the abrupt change of response upon failure start, as shown in **Fig.10**. This change in response can be more illustrated if lines corresponding to the ideal response of rods with different V_f are drawn as in **Fig.15**. When the failure starts, and in view of the mechanism above, the debonding causes reduction in the effective V_f and the response follows another line of lower V_f. This drop might take place several times depending on the failure path within the rod, and its detection is a function of the propagation speed.

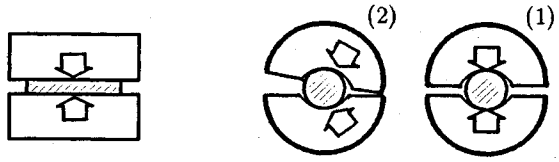

Fig.16 Stress Intensification due to Wedges rotation

A question arises here about the reason that drives rods follow one of the two mechanisms above. As the early failure initiation is induced by the lateral pressure of the grips, investigation of the grips becomes essential. A cross-section within the grips is shown in **Fig.16**, for both rods and standard specimens (with rectangular section as those for matrix specimens). In case of the standard specimens, the pressure from the grips is always uniform on the section due to the straight interface between the grips and the specimen. In case of the rods, the pressure is usually non-uniform due to the curved interface (1), and more stress concentration (2) is probable due to mis-settings or wedges rotation during loading, because of end coating roughness. This leads to early matrix failure at the highly stressed region and results in the the second

mechanism above.

It remains to compare the strength of the rods, concluded from the rule of mixture with that of the high peak. The rule of mixture in its approximate form (neglecting matrix strength) is

$$\sigma_c = V_f \sigma_f \quad \cdots\cdots (3)$$

where σ_c = composite strength
σ_f = fibers strength
V_f = fibers volume fraction

The value of σ_f is taken as the mean value of fibers strengths because it usually represents the stresses in the fibers at the failure of carbon fiber composites[10]. The application of the above rule for the case of carbon fibers leads to strength of 220 kg/mm^2 which is bigger than that of the high peak. This reduction in strength, however, is reasonable due to the additional axial stresses resulting from the lateral stresses at the grips. Detailed analysis of the stresses in both fibers and matrix is not the scope of this paper. However, a similar problem solved for homogeneous isotropic material is recalled. Barton[1] studied the problem of cylinder subjected to uniform pressure on a finite length of its surface and gave the distributions of axial stresses and lateral displacements resulting from this lateral pressure. The results for loaded lenghts of one and two times the cylinder diameter (a) are shown in **Fig.17** (a & b). Our case, however, is not a uniform surface pressure but rather uniform surface displacement due to the big difference in the lateral stiffness of the rod and the grips. The distribution of the surface pressure for this latter case was given also by Barton[1] and shown in **Fig.17** (c) over a loaded length a. The values are given in proportion to the central one p_0. The profile can be considered uniform, specially for the cases of longer loaded length (in the case of the rods, the loaded length is 16 a). It is expected that the effect of the lateral pressure will increase, in case of composites, because of the low modulus matrix that increases lateral displacement of fibers and hence the additional axial stresses.

Another source of this strength reduction might be the failure of the matrix in the case of the high peak too ; where the lateral pressure, though free of concentrations, becomes bigger and resembles the highly stressed zone in the case of the low peak. Matrix failure leads to shear, crushing of the fibers or simply failure extension of matrix cracks to the adjacent fibers those are sensitive to surface defects. Reduction of strength of continuous carbon fiber reinforced cement mortar, to about 50 % of that obtained from the rule of mixture, was reported[7]. This confirms the suggestion above, considering the brittleness of the mortar.

5. CONCLUSIONS

1. Fibers breakage during CFRP rods stretching, before failure, occurs in a very small percentage so that the strains are uniform along the rod. This gives reliability to the strains measured by short strain gages at rod center.
2. The lateral pressure from the gripping chucks plays an important role reducing rods strength due to the additional axial stresses induced at the chucks exit. It could, also, result in the failure of certain rod portion in crushing and/or shear modes leading to early failure of the rod.
3. Matrix strain capacity affects the process of failure initiation at the grips and participates to strength reduction. Brittle matrices could cause early failure in shear mode, under lateral pressure, and results in low tensile strength of the rods.

ACKNOWLEDGEMENT

The authors are quite grateful to TEIJIN ltd. for providing the tested fibers, matrix specimens and useful information about them.

REFERENCES

1) Barton, M. : The Circular Cylinder with a Band of Uniform Pressure on a Finite Length of Surface, *J. Appl. Mech.*, Vol.8, pp.A 97~A 104, Sept.1941.
2) Bhagwan, D.A. and Lowrence, J.B. : Analysis and Performance of Fiber Composites, John Wiley & Sons, 1980.
3) Hodhod, H. and Uomoto, T. : Experimental Model for Ideal Tensile Failure of FRP Rods, *JCI Proceedings*, Vol.13, No.1, pp.975~980, 1991.
4) Jayatilaka, S. : Fracture of Engineering Brittle Materials, Applied Science Publisher LTD., London, 1979.
5) Kobayashi, K. : Anchors for Fiber Reinforced Plastics Tendons for Prestressed Concrete, *Seiken Leaflet*, No.158, 1978 (In Japanese).
6) Poritsky, H. and Horvay, G. : Stress in Pipe Bundels, *J. Appl. Mech.*, Vol.13, pp.241~250, Sept. 1951.
7) Ramachendran, V.S., Feldman, R.F. and Beaudoin, J.J. : Concrete Science, Heyden, London, 1981.
8) Uomoto, T. and Nishimura, T. : Properties of Fiber Reinforced Plastic Rods for Prestressing Tendons of Concrete (1) ; Tensile Strength and Variation, *Seisan Kenkyu* : Journal of Institute of Industrial Science, University of Tokyo, Vol.42, pp.28~31 (In Japanese).
9) Weibull, W. : A Statistical Distribution Function of Wide Applicability, *J. Appl. Mech.*, Vol.13, pp.293 ~ 297, Sept.1951.
10) Watt, W. and Perov, B.V. : Handbook of Composites, Vol.1 : Strong Fibers, Elsevier Science Publishers B.V., Netherland, 1985.

(Received April 1. 1991)

Proc. of JSCE No. 451/V-17, pp. 245～253, August 1992

CFRPロッドの引張強度に及ぼす定着部の応力状態とマトリックスの品質の影響

ホドホド ホッサム・魚本健人

本研究はCFRPロッドをコンクリート用補強材として用いるために，既往の研究でその引張強度分布が2つのピークを持つと報告された原因を明らかにすることを目的とする．炭素繊維及びマトリックスの強度変形特性をそれぞれ実験で調べ，ロッドでは混合則が成立すること，既往の結果は定着部のロッドに対する軸直角方向の支圧力による表層部繊維の付加応力が原因となり，理論強度より低い荷重で破壊したためであることを明らかにした．